Mechanisms contributing to central excitability changes during hearing loss

Nadia Pilati[a], Matias J. Ison[b], Matthew Barker[a], Mike Mulheran[c], Charles H. Large[d], Ian D. Forsythe[a], John Matthias[e], and Martine Hamann[a,1]

[a]Department of Cell Physiology and Pharmacology and [c]Medical and Social Care Education, University of Leicester, Leicester LE19HN, United Kingdom; [b]Department of Engineering, University of Leicester, Leicester LE17RH, United Kingdom; [d]Autifony Therapeutics Limited, Medicines Research Centre, 37135 Verona, Italy; and [e]School of Art and Media, Faculty of Arts, Plymouth University, Devon PL48AA, United Kingdom

Edited by Roger A. Nicoll, University of California, San Francisco, CA, and approved March 30, 2012 (received for review October 14, 2011)

Exposure to loud sound causes cochlear damage resulting in hearing loss and tinnitus. Tinnitus has been related to hyperactivity in the central auditory pathway occurring weeks after loud sound exposure. However, central excitability changes concomitant to hearing loss and preceding those periods of hyperactivity, remain poorly explored. Here we investigate mechanisms contributing to excitability changes in the dorsal cochlear nucleus (DCN) shortly after exposure to loud sound that produces hearing loss. We show that acoustic overexposure alters synaptic transmission originating from the auditory and the multisensory pathway within the DCN in different ways. A reduction in the number of myelinated auditory nerve fibers leads to a reduced maximal firing rate of DCN principal cells, which cannot be restored by increasing auditory nerve fiber recruitment. In contrast, a decreased membrane resistance of DCN granule cells (multisensory inputs) leads to a reduced maximal firing rate of DCN principal cells that is overcome when additional multisensory fibers are recruited. Furthermore, gain modulation by inhibitory synaptic transmission is disabled in both auditory and multisensory pathways. These cellular mechanisms that contribute to decreased cellular excitability in the central auditory pathway are likely to represent early neurobiological markers of hearing loss and may suggest interventions to delay or stop the development of hyperactivity that has been associated with tinnitus.

auditory brainstem | fusiform cell | parallel fiber | deafness | whole-cell patch

It is well established that exposure to loud sound causes damage to the cochlea and results in an elevation of hearing thresholds (1) often accompanied by a reduction of auditory nerve (AN) firing rate (2–4). Although peripheral cellular mechanisms contributing to hearing loss have been thoroughly described (5–11), mechanisms in the central auditory system involved in the early stages of hearing loss following acoustic overexposure (AOE) are poorly understood. The dorsal cochlear nucleus (DCN) is one of the first relays within the central auditory pathway (12). Hyperactivity in the DCN has been reported weeks after AOE in vivo and in brain slices and has been correlated with tinnitus (13–15). Our recent study showed the presence of bursts in DCN fusiform cells (FCs) just a few days after AOE (16). Therefore, the aim of the current study was to investigate synaptic transmission at this early time point after AOE and determine whether changes in auditory or multisensory (MS) inputs to FCs might contribute to the altered excitability in the DCN. We postulate that changes following AOE could represent the earliest modifications of the central auditory pathway preceding the later development of DCN hyperactivity and tinnitus. DCN FCs integrate the acoustic information from AN fibers with MS signals transmitted via granule cell axons (parallel fibers) (17–19). DCN granule cells and their parallel fiber axons represent a site of integration of multimodal sensory inputs such as the trigeminal ganglion (20), the spinal trigeminal nucleus (21), the pontine nucleus (22), the cuneate nucleus, the gracile nuclei (23, 24), and the raphe nucleus (25). These inputs are likely to encode proprioceptive information on the position of the ears relative to the sound source (26) and/or the suppression of body-generated sounds or vocal feedback (17, 27, 28). Responses of FCs are further shaped by feed-forward inhibition, mainly through inhibitory tuberculo-ventral cells activated by AN fibers and cartwheel cells activated by parallel fibers (17, 29–31). Consequently, the changes in intrinsic excitability and spontaneous activity of FCs following AOE (16) may arise as a consequence of specific changes occurring along the AN and the MS pathway after AOE. The way in which a neuron processes signals can be captured by its transfer function or its input–output relationship (32). Modulation of excitability changes the shape of this relationship, thereby affecting either the slope (or gain) or its maximum (33–35). We therefore used FC transfer functions to target central excitability changes after AOE. Our experimental and computational modeling studies show that synaptic excitability is down-regulated in FCs during hearing loss, at the early stages following AOE, and that the underlying cellular mechanisms are specific to the AN and MS synaptic inputs.

Results

Acoustic Overexposure Induces Hearing Threshold Elevations and Decreases FC Excitability. We assessed the effects of AOE on auditory brainstem responses (ABR) for frequencies varying from 8 to 30 kHz. Wistar rats aged 15–18 d were subjected to 110 dB sound pressure level (SPL), 14.8 kHz for 4 h, and ABR were recorded 3–4 d later. There were no changes in ABR threshold and latencies measured at day 0 and day 3–4 in control animals (Fig. S1*C* and Table S1). We found that shifts of hearing thresholds of 20–30 dB SPL were observed for frequencies above the frequency used during the AOE protocol (Fig. S1 *A*–*C*) whereas wave 1 and 2 latencies were unaffected (Tables S2 and S3). ABR threshold shifts were temporary as they recovered after 3 mo (Fig. S1*C*). Whole-cell current clamp recordings from DCN FCs in vitro were then performed at a similar time (3–4 d) after AOE or after a sham procedure with anesthesia only (unexposed). Excitatory post-synaptic potentials (EPSPs) and action potentials (APs) could be elicited in FCs after stimulating the AN in the DCN deep layer (19, 36, 37) (*SI Methods* and Fig. 1 *A*–*C*) or MS inputs in the DCN molecular layer (37, 38) (Fig. 1 *D*–*F*). AOE led to reduction of the EPSPs evoked by AN and MS input stimulations [from 8 ± 1 mV (n = 5) to 4 ± 1 mV (n = 6) in unexposed conditions and after AOE, respectively ($P < 0.01$, unpaired t test) (Fig. 1*B*) and from 6 ± 1 mV (n = 8) to 1.5 ± 0.5 mV (n = 6) in unexposed conditions and AOE, respectively ($P <$

Author contributions: M.H. designed research; N.P. and M.B. performed research; M.J.I., M.M., and J.M. contributed new reagents/analytic tools; N.P., M.J.I., and M.B. analyzed data; and N.P., C.H.L., I.D.F., and M.H. wrote the paper.

The authors declare no conflict of interest.

This article is a PNAS Direct Submission.

Freely available online through the PNAS open access option.

[1]To whom correspondence should be addressed. E-mail: mh86@le.ac.uk.

This article contains supporting information online at www.pnas.org/lookup/suppl/doi:10.1073/pnas.1116981109/-/DCSupplemental.

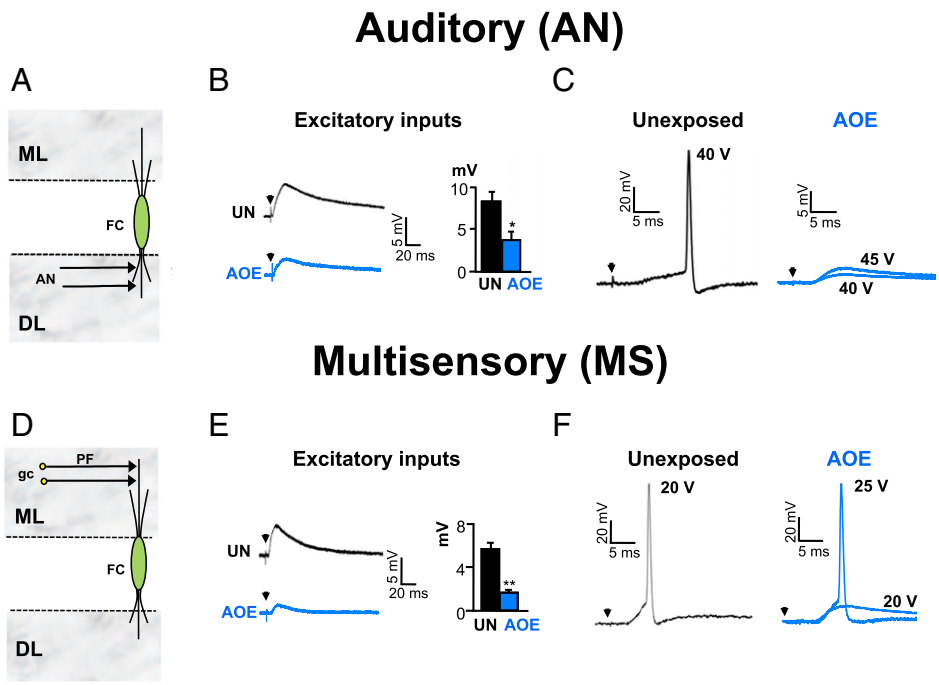

Fig. 1. AOE down-regulates AN and MS synaptic transmission to FCs. (*A*) AN inputs directly terminate onto FC basal dendrites in the deep layer (DL). (*B*) AN stimulations (25 V, 0.3 Hz) trigger smaller EPSPs after AOE (blue). Membrane potential was −70 mV. Histogram summarizes EPSP amplitudes measured at similar stimulating voltages in unexposed (25 ± 4 V, $n = 4$) and exposed conditions (28 ± 2 V, $n = 6$). (*C*) In unexposed condition (black), AN stimulations (40 V, 0.3 Hz) trigger action potentials in a FC (membrane potential of −60 mV). After AOE (blue), AN stimulations (40–45 V, 0.3 Hz) fail to trigger action potentials. (*D*) MS inputs originate from parallel fibers (PF), which are the granule cell (gc) axons terminating onto FC apical dendrites in the molecular layer (ML). (*E*) MS stimulations (15 V, 0.3 Hz) trigger smaller EPSPs after AOE (blue). Membrane potential was −70 mV. Histogram summarizes EPSP amplitudes measured at similar stimulating voltages in unexposed (16 ± 1 V, $n = 8$) and exposed conditions (19 ± 2 V, $n = 6$). (*F*) In unexposed condition (black), MS stimulations (20 V, 0.3 Hz) trigger action potentials in a FC (membrane potential of −60 mV). After AOE (blue), higher stimulation voltages (25 V, 0.3 Hz) are required to trigger an action potential. *$P < 0.05$, **$P < 0.01$: unpaired *t* tests.

0.01 unpaired *t* test) (Fig. 1*E*)]. Furthermore, after AOE, stimulation of the AN inputs was unable to trigger APs even with higher stimulating voltages (Fig. 1*C* and Table S4). By contrast, APs could be elicited by stimulation of the MS inputs after AOE, but higher stimulating voltages were then required (Fig. 1*F*).

AOE Reduces FC Maximal Firing Rate upon AN Stimulations and Decreases the Number of Myelinated AN Fibers in the Cochlea. Inputs to FCs were stimulated over a range of frequencies (10–100 Hz) and intensities (from threshold to suprathreshold voltages ranging from 20 to 50 V) to proceed to a temporal and spatial recruitment of the EPSPs, respectively. FC input–output relationships were quantified by fitting the data to Hill-like equations (39, 40) and by measuring the change in the slope and in the maximal firing rate (*SI Methods*). Whereas single stimuli of AN inputs were unable to trigger APs in FCs after AOE, firing could now be evoked by trains of stimuli ranging from 10 to 100 Hz. Input–output functions were performed by increasing stimulus voltage to recruit AN fibers and allow fiber recruitment at suprathreshold voltages (Fig. 2*A* and Fig. S2*A*). FC maximal firing rate following AN input stimulation was reduced from 85 ± 7 Hz ($n = 5$) to 49 ± 6 Hz ($n = 5$); $P < 0.05$ after AOE (Fig. 2*A*, blue). This was observed at similar threshold (Fig. S2 *A* and *B*) and suprathreshold (Fig. 2*A* and Fig. S2 *A* and *B*) stimulating voltages. These data were reproduced using a Leaky Integrate and Fire model implemented in MATLAB (Mathworks) (*SI Methods*, Fig. 2*A*, and Table S5), and the effects of AOE on the FC transfer function following AN stimulation were reproduced by reducing the number of available AN fibers by ~50%. We subsequently used transmitted electron microscopy (TEM) (*SI Methods*) to test whether AOE led to a demyelination of AN fibers giving rise to the "unrecoverable" deficit in AN transmission observed by increasing stimulus voltage (Figs. 1*C* and 2*A*). In unexposed animals, 90 ± 5.0% ($n = 10$) of AN fibers within the cochlea were myelinated whereas the remaining 10.4 ± 5.0% ($n = 10$) were non-myelinated. This was consistent with the proportion of type I myelinated and type II non-myelinated AN fibers described in previous studies (41). The total number of AN fibers remained unaffected after AOE [50 ± 6 per 400 μm^2 ($n = 8$) in the unexposed condition and 49 ± 7 per 400 μm^2 ($n = 8$), $P > 0.05$]. However, the proportion of myelinated AN fibers decreased by about half after AOE [to reach 50 ± 1.5% of control levels ($n = 10$), $P < 0.001$ (Fig. 2*B*)], and this effect was specifically observed at the base of the cochlea involved in processing high-frequency sound (42, 43). Conversely, the proportion of non-myelinated AN fibers increased by about a factor of 4 at the base of the cochlea [to reach 50 ± 3.1% of the total number of AN fibers ($n = 10$), $P < 0.001$]. After AOE, the internal diameters of myelinated and non-myelinated AN fibers at the base were similar [1.60 ± 0.11 μm ($n = 32$) and 1.57 ± 0.10 μm ($n = 32$), respectively; $P > 0.05$], indicating that there is loss of myelin around type I fibers, giving them the appearance of type II fibers. When a 50% reduction in the number of myelinated AN fibers was implemented in the model, it reproduced the transfer function obtained after AOE (Fig. 2*A*). This suggests that the decreased excitability evoked by AN inputs as well as the reduced EPSP amplitudes (Fig. 1*B*) are due to a lower proportion of myelinated AN fibers within the cochlea after AOE. Both ABR thresholds (Fig. S1*C*) and percentage of myelinated AN fibers (Fig. S1*D* and Table S6) recovered 3 mo after AOE. In conclusion, after AOE, FCs were unable to fire at frequencies exceeding 50 Hz, due to a reduced number of conducting AN fibers. This accounts for the apparent deficit in FC excitability, which could not be restored by increasing AN input stimulation. Movie S1 models the firing times of the FC stimulated

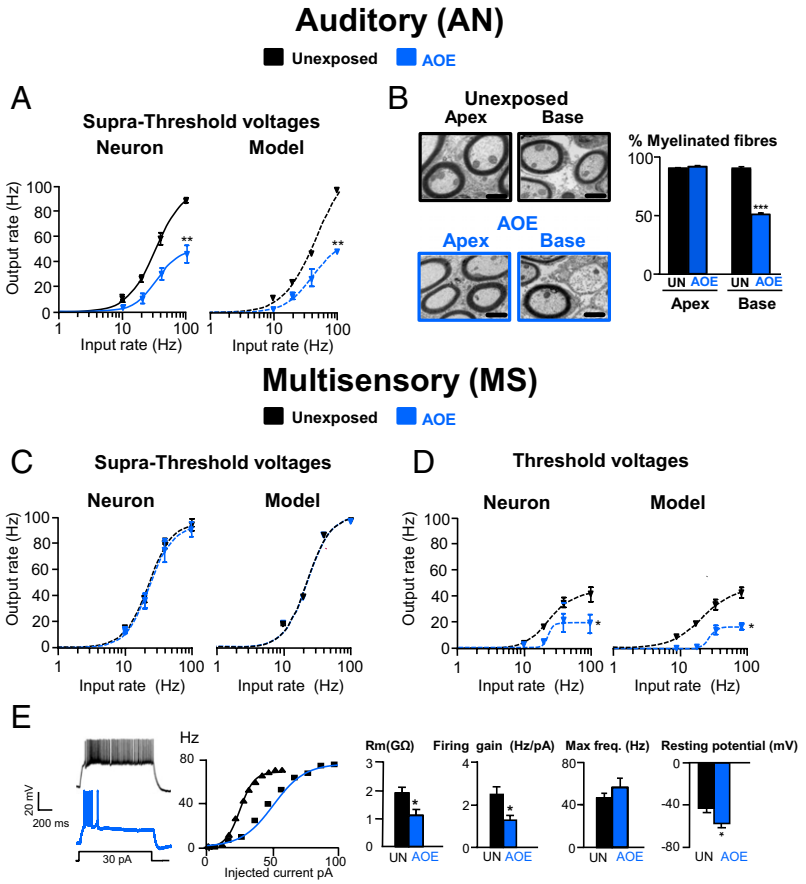

Fig. 2. AOE modulates FC transfer function upon AN and MS stimulation. (*A*) AN inputs were stimulated from 10 to 100 Hz. Average input–output relationships (n = 5–6) were obtained in unexposed condition (black) and after AOE (blue). Experimental and model data are represented, and lines are fits to a Hill function as detailed in *SI Methods*. (*B*) Transmitted electron micrographs of peripheral AN fibers in control condition (black frame) and after AOE (blue frame) at the base and the apex of the cochlea. Histograms represent the percentage of myelinated AN fibers in those conditions. (Scale bar: 1 μm.) (*C* and *D*) MS inputs (n = 5–6) were stimulated, and experimental and model data were fitted as described in *A*. Firing frequencies were measured at suprathreshold (*C*) and threshold (*D*) stimulating voltages. (*E*) Traces represent the granule cell firing in response to 1-s, 30-pA step current injections in unexposed condition (black) and after AOE (blue). Transfer functions for the two cells are shown. Histograms show that AOE decreases the granule cell membrane resistance and firing gain, leaving the maximal firing frequency unaffected (n = 9–10 per condition). Granule cell resting potentials were more hyperpolarized after AOE. $*P < 0.05$, $**P < 0.01$, $***P < 0.001$: unpaired t tests.

at 50 Hz by AN inputs and shows a notable decrease in firing frequency at threshold and suprathreshold voltages after AOE.

AOE Reduces FC Maximal Firing Rate upon MS Input Stimulation and Decreases Granule Cell Membrane Resistance. In contrast to AN stimulation, the FC maximal firing rate following MS input stimulation was completely preserved at suprathreshold stimulating voltages with FCs still capable of firing 88 ± 9 Hz (n = 6) Hz after AOE [versus 93 ± 11 Hz (n = 6) in an unexposed condition (Fig. 2*C* and Fig. S2 *C* and *D*)]. However, when MS inputs were stimulated at threshold voltages to induce minimal fiber recruitment, the FC maximal firing rate was significantly reduced after AOE [from 45 ± 11 Hz (n = 6) to 16 ± 6 Hz (n = 6), $P < 0.05$ (Fig. 2*D* and Fig. S2 *C* and *D*)]. As previously, these data could be reproduced using the Leaky Integrate and Fire model, but in this case a good fit required the membrane resistance of the MS inputs to be reduced by half (Fig. 2 *C* and *D* and Table S7) without changing their total number, in contrast to the above results. As MS inputs to DCN FCs are carried by granule cell axons (44), we directly recorded from DCN granule cells to characterize their passive and active membrane properties. Granule cell spontaneous firing rate was unaffected by AOE (Fig. S3 and Table S8). Nevertheless, we found that AOE decreased their membrane resistance [from 1.9 ± 0.3 GΩ (n = 7) to 1.1 ± 0.2 GΩ (n = 10), $P < 0.05$ (Fig. 2*E*)], which led to more hyperpolarized resting potentials [from −43 ± 4 mV (n = 7) to −57 ± 4 mV (n = 10), $P < 0.05$ (Fig. 2*E*)]. Membrane resistance values implemented in the model allowed the reproduction of the transfer functions obtained in control conditions and after AOE (Fig. 2 *C* and *D* and Table S7). The reduction of granule cell membrane resistance after AOE is consistent with values implemented in the modeling. Moreover, we found that the granule cell firing gain was decreased after AOE [from 2.5 ± 0.4 Hz/pA (n = 10) to 1.4 ± 0.2 Hz/pA after AOE (n = 9), $P < 0.05$ (Fig. 2*E*)], and this explains the FC decreased excitability at threshold voltages. However, after AOE, granule cell maximal firing remained unaffected (Fig. 2*E*), which explains how the FC maximal firing rate was preserved at suprathreshold stimulating voltage (when granule cells were firing at their maximal rate). Movie S1 models the firing times of the FC stimulated at 50 Hz following MS stimulation. The firing (beat) frequency is decreased at threshold voltages, whereas it is preserved at suprathreshold voltages. This contrasts to AN firing frequency after AOE where the firing frequency is decreased at both threshold and suprathreshold voltages.

Inhibitory Synaptic Transmission Modulates FC Firing Gain. Modulation of the sensitivity or gain of neural responses to input is an

important component of neural computation (34, 35). Inhibitory synaptic transmission changes the slope of the input–output relationships, thereby modulating the gain of the cell transfer function (40, 45). We subsequently studied whether inhibitory synaptic transmission controls gain modulation in the DCN. Both AN and MS synaptic inputs activate inhibitory interneurones projecting onto FC basal and apical dendrites, respectively (Fig. 3 *A* and *C*) (17). FC transfer functions (following AN and MS stimulation) were obtained in control medium or in the presence of strychnine and gabazine (to block inhibitory synaptic transmission) and changes in the slope (gain) were quantified. We found that inhibitory synaptic transmission was most effective while stimulating AN inputs to FCs and decreased the maximal firing rate by two- to threefold (Fig. 3*E*). Blocking inhibitory synaptic transmission during AN stimulation also increased the firing gain by about 70% (Fig. 3*E*). In contrast, inhibitory synaptic transmission produced only a modest scaling down during MS stimulation at threshold voltages [minimal fiber recruitment (Fig. 3*F*, *Left*)] whereas no changes were observed at higher stimulating voltages (Fig. 3*F*, *Right*). This was also reflected in the size of the inhibitory postsynaptic potentials (IPSPs), which was doubled when elicited by AN stimulation compared with MS input stimulation (Fig. 3 *B* and *D*, Histograms in black). These data indicate that inhibitory synaptic transmission modulating gain in the DCN occurs mainly via activation of AN inputs.

AOE Disables FC Gain Control by Inhibitory Synaptic Transmission. Given that EPSPs elicited upon AN and MS input stimulation were down-regulated after AOE and that inhibitory synaptic transmission into FCs is dependent on those inputs, we asked whether inhibitory synaptic transmission is also down-regulated after AOE. To address this question, we measured the IPSPs evoked by AN and MS input stimulation and found that both were significantly decreased [from 4.2 ± 0.7 mV (n = 4) to 1.5 ± 0.3 mV (n = 5), $P < 0.01$, and from 1.9 ± 0.4 mV (n = 8) to 0.3 ± 0.2 mV (n = 6), $P < 0.01$, respectively (Fig. 3 *B* and *D*)]. We next examined whether the decreased IPSP size was affecting the transfer function in FCs. We found that, after AOE, inhibitory synaptic transmission failed to modulate the FC firing gain following AN or MS input stimulations (Fig. 3*G*, *Right* and *H*). Moreover, after AOE, inhibitory inputs reduced the FC maximal firing rate evoked by AN stimulation (Fig. 3*G*) but not by MS stimulation (Fig. 3*H*). Data were reproduced using the Leaky Integrate and Fire model (Fig. S4) employing the same parameters as previously described (Tables S5 and S7) and decreasing the strength of inhibitory synapses (to match the down-regulation of IPSPs shown in Fig. 3 *B* and *D*).

Discussion

Reduced auditory nerve activity within the peripheral system after AOE has been previously reported (1, 4, 46, 47). Our results reveal the cellular mechanisms underlying a decrease of cellular

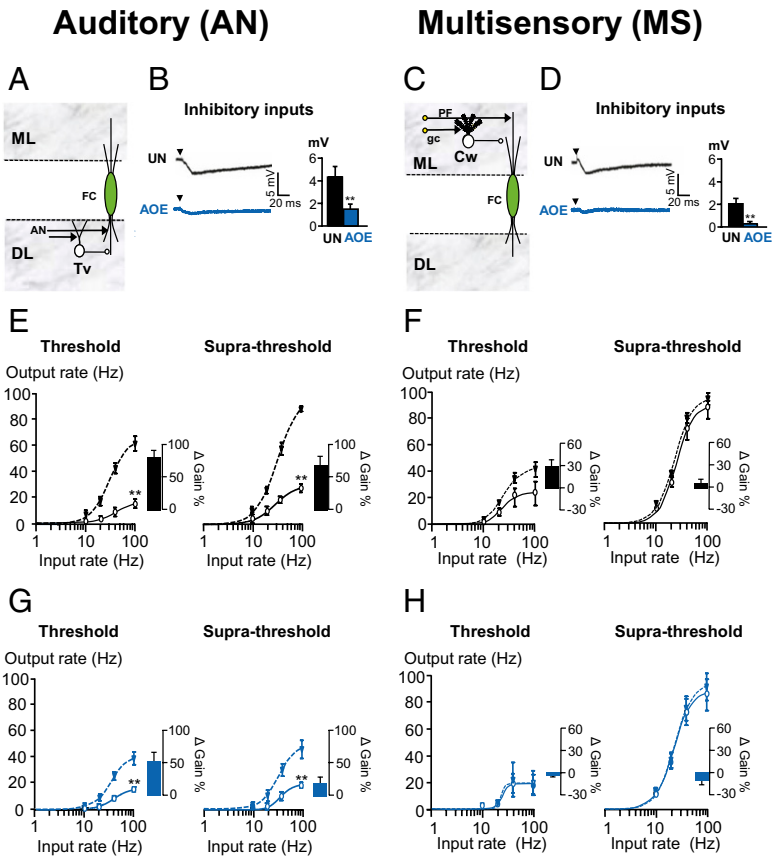

Fig. 3. FC gain control via inhibitory synaptic transmission is disabled after AOE. (*A*) AN inputs directly terminate in tuberculo ventral cells (Tv), which inhibit FCs. (*B*) AN stimulations (25 V, 0.3 Hz) trigger smaller IPSPs after AOE (blue). Membrane potential was −70 mV. (*C*) MS inputs directly terminate onto cartwheel cells (Cw), which inhibit FCs. (*D*) MS stimulations (25 V, 0.3 Hz) trigger smaller IPSPs after AOE (blue). Membrane potential was −70 mV. (*E–H*) Average input–output relationships (n = 5–6) were obtained following AN (*E* and *G*) and MS (*F* and *H*) stimulations before (solid line) and after (dashed line) removal of synaptic inhibition. (*G*) Note that inhibitory synaptic transmission has a reduced modulatory effect at threshold which disappears at supra-threshold stimulating voltages. Experimental data are represented in control (*E* and *F*) and after AOE (*G* and *H*), and lines are fits to a Hill function as detailed in *SI Methods*. Histograms represent the changes in the gain before and after removal of synaptic inhibition. **$P < 0.01$: unpaired t tests.

excitability that occurs in the central auditory pathway during the period of initial hearing-threshold elevation triggered by AOE. The major finding of this study is that AN and MS synaptic transmission is differently affected by loud sound exposure. Although we cannot exclude the possibility that deafferentation due to the slicing procedure might lower the synaptic excitability, this is unlikely to be the reason for the effects that we observed after AOE, as we would expect deafferentation to affect excitability similarly in unexposed and exposed conditions. Our EM studies demonstrate that the proportion of AN fibers that were myelinated was reduced by half after AOE, consistent with a loss of efficiency in initiating and propagating action potentials along the AN fibers following electrical stimuli (41). This correlates with previous morphological studies showing a reduced number of myelinated central processes within the modiolus following deafening (48, 49). Demyelination of the AN is also reported in sensorineural deafness (42) and has been suggested to play a role in auditory neuropathy (50), a hearing disorder characterized by absent auditory brainstem responses with preserved outer hair cell function. Myelin disruption results in increased membrane time constants, decreased conduction velocity (51), and decreased membrane resistance (52, 53), all of which could lead to conduction block (54). Conduction block could result in failure of transmitter release at the pathologically unmyelinated AN terminals, and this could explain why FC maximal firing could not be achieved even when stimulating at amplitudes allowing maximal AN fiber recruitment. The loss of action potential propagation along the AN fibers may also explain the auditory brainstem response threshold elevations, similar to AN myelinopathy (50). As ABR thresholds are affected, this could be due to AN fibers with low threshold and high spontaneous rate being primarily affected (11).

Concomitant to the effects observed in AN fibers, a decreased membrane resistance contributes to the decreased excitability of granule cells, reducing their synaptic output for a given input, which presumably accounts for the reduced responsiveness of FCs to MS stimulation. However, in contrast to AN fiber activation, granule cell maximal firing frequency was preserved after AOE, which explains why FC excitability to MS input stimulation was preserved although requiring higher stimulating voltages. The selective effects on FC transfer functions at low stimulating voltage were reproduced by our modeling study, which supports the proposal that the change in granule cell membrane resistance was the major contributor to alteration of FC transfer function after AOE. Decreased membrane resistance observed in granule cells could arise through increased function or expression of two-pore domain "leak" K^+ channels that would also account for the hyperpolarized resting potential (55, 56) observed in our study. Further supporting this hypothesis, deafness has been shown to be associated with changes in the expression of two-pore domain K^+ channels in the cochlear nucleus (57). Inhibitory synaptic transmission plays a major role in gain modulation within the CNS (40, 45), and we have shown that this type of modulation also occurs in the AN and MS pathways within the DCN. We have shown that inhibitory synaptic transmission plays a major role in the AN transfer function modulation. We have also found that inhibitory synaptic transmission was ineffective in controlling FC transfer function when stimulating MS inputs with high voltages and that this is likely to be due to the recruitment of excitatory inputs originating from parallel fibers overcoming the effects of inhibitory synaptic transmission. After AOE, inhibition-mediated gain increases were absent following MS and AN stimulations, and this could be explained by the down-regulation of IPSPs recorded in FCs observed in both AN and MS synaptic pathways. A loss of inhibition was also observed following unilateral cochlear ablation (58, 59), and a decrease in glycine receptor expression in the DCN after AOE has been previously reported (60). In vivo studies have shown reduced spontaneous activity in the DCN a few days after acoustic overexposure (61). This was then followed at 3 wk post AOE by an elevated activity in the DCN (61, 62), which has been associated with the perception of tinnitus (14, 63, 64). The latest computational modeling studies predict that decreased AN activity following damage to the cochlea is then counteracted by an increase of the response gain of neurons in the DCN, which restores the mean firing rate but also leads to hyperactivity in the DCN (65). The reduced synaptic excitability in DCN FCs observed in the present study could therefore represent a first step in triggering homeostatic plastic adjustments that lead to hyperactivity and tinnitus (14, 64–67). Hyperactivity related to tinnitus could result from a simultaneous reduction of AN-mediated transmission and an enhanced MS-mediated transmission (68) and/or a reduction in inhibitory synaptic transmission (58–60, 67). Furthermore, the MS input excitability increase observed weeks after AOE (68) could represent a compensatory mechanism to counteract the initial MS-reduced excitability described in this paper. In conclusion, our study shows that excitability changes in the DCN can be mechanistically unraveled and provides insights into neurobiological markers following acoustic overexposure that trigger or result from shifts of hearing threshold. These insights may allow the design of pharmaceutical or other manipulations that could delay or stop the progression to tinnitus following acoustic trauma in humans.

Methods

For detailed information on the animals, ABR, and the neuronal model used, see *SI Methods*.

AOE. Two sessions of 2 h of AOE (110 dB SPL, 14.8 kHz) were performed at P15–P18, which corresponds to the period after hearing onset (70) See *SI Methods* for more detailed information.

Whole-Cell Current Clamp Recordings. These recordings were performed from FCs and granule cells in coronal brainstem slices (170 μm) containing the dorsal cochlear nucleus (Fig. S5).

Statistical Analysis. Data are presented as mean ± SEM, and statistical comparisons were performed by unpaired or paired two-tailed Student's *t* tests. A significance level of $P < 0.05$ was adopted throughout.

ACKNOWLEDGMENTS. We thank B. Billups and C. Kopp-Scheinpflug for comments on the manuscript; N. Allcock for help with the electron microscopy; and M. Berti and J. Solinski for help with the 3D reconstruction of the DCN. This research was supported by Wellcome Trust, GlaxoSmithKline, the Royal Society, and MediSearch (UK).

1. Liberman MC, Dodds LW (1984) Single-neuron labeling and chronic cochlear pathology. III. Stereocilia damage and alterations of threshold tuning curves. *Hear Res* 16(1): 55–74.
2. Liberman MC, Dodds LW (1984) Single-neuron labeling and chronic cochlear pathology. II. Stereocilia damage and alterations of spontaneous discharge rates. *Hear Res* 16(1):43–53.
3. Shepherd RK, Roberts LA, Paolini AG (2004) Long-term sensorineural hearing loss induces functional changes in the rat auditory nerve. *Eur J Neurosci* 20:3131–3140.
4. Sly DJ, et al. (2007) Deafness alters auditory nerve fibre responses to cochlear implant stimulation. *Eur J Neurosci* 26:510–522.
5. Pujol R, Puel J-L (1999) Excitotoxicity, synaptic repair, and functional recovery in the mammalian cochlea: A review of recent findings. *Ann N Y Acad Sci* 884:249–254.
6. Ruel J, et al. (2007) Physiology, pharmacology and plasticity at the inner hair cell synaptic complex. *Hear Res* 227(1–2):19–27.
7. Han Y, et al. (2011) Up-regulation of Nob1 in the rat auditory system with noise-induced hearing loss. *Neurosci Lett* 491(1):79–82.
8. Bodmer D (2008) Protection, regeneration and replacement of hair cells in the cochlea: Implications for the future treatment of sensorineural hearing loss. *Swiss Med Wkly* 138:708–712.
9. Canlon B (1988) The effect of acoustic trauma on the tectorial membrane, stereocilia, and hearing sensitivity: Possible mechanisms underlying damage, recovery, and protection. *Scand Audiol Suppl* 27:1–45.
10. Kujawa SG, Liberman MC (2009) Adding insult to injury: Cochlear nerve degeneration after "temporary" noise-induced hearing loss. *J Neurosci* 29:14077–14085.

11. Lin HW, Furman AC, Kujawa SG, Liberman MC (2011) Primary neural degeneration in the Guinea pig cochlea after reversible noise-induced threshold shift. *J Assoc Res Otolaryngol* 12:605–616.
12. Cohen ES, Brawer JR, Morest DK (1972) Projections of the cochlea to the dorsal cochlear nucleus in the cat. *Exp Neurol* 35:470–479.
13. Chang H, Chen K, Kaltenbach JA, Zhang J, Godfrey DA (2002) Effects of acoustic trauma on dorsal cochlear nucleus neuron activity in slices. *Hear Res* 164(1–2):59–68.
14. Kaltenbach JA (2007) The dorsal cochlear nucleus as a contributor to tinnitus: Mechanisms underlying the induction of hyperactivity. *Prog Brain Res* 166:89–106.
15. Middleton JW, et al. (2011) Mice with behavioral evidence of tinnitus exhibit dorsal cochlear nucleus hyperactivity because of decreased GABAergic inhibition. *Proc Natl Acad Sci USA* 108:7601–7606.
16. Pilati N, Large C, Forsythe ID, Hamann M (2012) Acoustic over-exposure triggers burst firing in dorsal cochlear nucleus fusiform cells. *Hear Res* 283(1–2):98–106.
17. Oertel D, Young ED (2004) What's a cerebellar circuit doing in the auditory system? *Trends Neurosci* 27(2):104–110.
18. Davis KA, Miller RL, Young ED (1996) Effects of somatosensory and parallel-fiber stimulation on neurons in dorsal cochlear nucleus. *J Neurophysiol* 76:3012–3024.
19. Zhang S, Oertel D (1994) Neuronal circuits associated with the output of the dorsal cochlear nucleus through fusiform cells. *J Neurophysiol* 71:914–930.
20. Shore SE, Vass Z, Wys NL, Altschuler RA (2000) Trigeminal ganglion innervates the auditory brainstem. *J Comp Neurol* 419:271–285.
21. Zhou J, Shore S (2004) Projections from the trigeminal nuclear complex to the cochlear nuclei: A retrograde and anterograde tracing study in the guinea pig. *J Neurosci Res* 78:901–907.
22. Babalian AL (2005) Synaptic influences of pontine nuclei on cochlear nucleus cells. *Exp Brain Res* 167:451–457.
23. Itoh K, et al. (1987) Direct projections from the dorsal column nuclei and the spinal trigeminal nuclei to the cochlear nuclei in the cat. *Brain Res* 400(1):145–150.
24. Weinberg RJ, Rustioni A (1987) A cuneocochlear pathway in the rat. *Neuroscience* 20:209–219.
25. Thompson AM, Moore KR, Thompson GC (1995) Distribution and origin of serotoninergic afferents to guinea pig cochlear nucleus. *J Comp Neurol* 351(1):104–116.
26. Kanold PO, Young ED (2001) Proprioceptive information from the pinna provides somatosensory input to cat dorsal cochlear nucleus. *J Neurosci* 21:7848–7858.
27. Shore SE (2005) Multisensory integration in the dorsal cochlear nucleus: Unit responses to acoustic and trigeminal ganglion stimulation. *Eur J Neurosci* 21:3334–3348.
28. Shore SE, Zhou J (2006) Somatosensory influence on the cochlear nucleus and beyond. *Hear Res* 216–217:90–99.
29. Golding NL, Oertel D (1997) Physiological identification of the targets of cartwheel cells in the dorsal cochlear nucleus. *J Neurophysiol* 78:248–260.
30. Voigt HF, Young ED (1990) Cross-correlation analysis of inhibitory interactions in dorsal cochlear nucleus. *J Neurophysiol* 64:1590–1610.
31. Rhode WS (1999) Vertical cell responses to sound in cat dorsal cochlear nucleus. *J Neurophysiol* 82:1019–1032.
32. Koch C (1999) *Biophysics of Computation: Information Processing in Single Neurons* (Oxford Univ Press, Oxford), pp 117–130.
33. Holt GRKC, Koch C (1997) Shunting inhibition does not have a divisive effect on firing rates. *Neural Comput* 9:1001–1013.
34. Salinas E, Thier P (2000) Gain modulation: A major computational principle of the central nervous system. *Neuron* 27(1):15–21.
35. Chance FS, Abbott LF, Reyes AD (2002) Gain modulation from background synaptic input. *Neuron* 35:773–782.
36. Osen KK (1970) Course and termination of the primary afferents in the cochlear nuclei of the cat. An experimental anatomical study. *Arch Ital Biol* 108(1):21–51.
37. Fujino K, Oertel D (2003) Bidirectional synaptic plasticity in the cerebellum-like mammalian dorsal cochlear nucleus. *Proc Natl Acad Sci USA* 100:265–270.
38. Tzounopoulos T, Kim Y, Oertel D, Trussell LO (2004) Cell-specific, spike timing-dependent plasticities in the dorsal cochlear nucleus. *Nat. Neurosci.* 7:719–725.
39. Murphy BK, Miller KD (2003) Multiplicative gain changes are induced by excitation or inhibition alone. *J Neurosci* 23:10040–10051.
40. Rothman JS, Cathala L, Steuber V, Silver RA (2009) Synaptic depression enables neuronal gain control. *Nature* 457:1015–1018.
41. Weisz CGE, Glowatzki E, Fuchs P (2009) The postsynaptic function of type II cochlear afferents. *Nature* 461:1126–1129.
42. Spoendlin H, Schrott A (1989) Analysis of the human auditory nerve. *Hear Res* 43(1): 25–38.
43. Yajima YaH, Hayashi Y (1989) Response properties and tonotopical organization in the dorsal cochlear nucleus in rats. *Exp Brain Res* 75:381–389.
44. Mugnaini E, Warr WB, Osen KK (1980) Distribution and light microscopic features of granule cells in the cochlear nuclei of cat, rat, and mouse. *J Comp Neurol* 191: 581–606.
45. Mitchell SJ, Silver RA (2003) Shunting inhibition modulates neuronal gain during synaptic excitation. *Neuron* 38:433–445.
46. Salvi RJ, Hamernik RP, Henderson D (1983) Response patterns of auditory nerve fibers during temporary threshold shift. *Hear Res* 10(1):37–67.
47. Schaette R, Kempter R (2009) Predicting tinnitus pitch from patients' audiograms with a computational model for the development of neuronal hyperactivity. *J Neurophysiol* 101:3042–3052.
48. Terayama Y, Kaneko K, Tanaka K, Kawamoto K (1979) Ultrastructural changes of the nerve elements following disruption of the organ of Corti. II. Nerve elements outside the organ of Corti. *Acta Otolaryngol* 88(1–2):27–36.
49. Hoeffding V, Feldman ML (1988) Degeneration in the cochlear nerve of the rat following cochlear lesions. *Brain Res* 449(1–2):104–115.
50. El-Badry MM, Ding DL, McFadden SL, Eddins AC (2007) Physiological effects of auditory nerve myelinopathy in chinchillas. *Eur J Neurosci* 25:1437–1446.
51. Franssen H (2008) Electrophysiology in demyelinating polyneuropathies. *Expert Rev Neurother* 8(3):417–431.
52. Brismar T (1981) Electrical properties of isolated demyelinated rat nerve fibres. *Acta Physiol Scand* 113(2):161–166.
53. Cragg BG, Thomas PK (1964) The conduction velocity of regenerated peripheral nerve fibres. *J Physiol* 171:164–175.
54. Bai Y, et al. (2010) Conduction block in PMP22 deficiency. *J Neurosci* 30:600–608.
55. Millar JA, et al. (2000) A functional role for the two-pore domain potassium channel TASK-1 in cerebellar granule neurons. *Proc Natl Acad Sci USA* 97:3614–3618.
56. Talley EM, Lei Q, Sirois JE, Bayliss DA (2000) TASK-1, a two-pore domain K+ channel, is modulated by multiple neurotransmitters in motoneurons. *Neuron* 25:399–410.
57. Holt AG, et al. (2006) Deafness associated changes in expression of two-pore domain potassium channels in the rat cochlear nucleus. *Hear Res* 216–217(June–July):146–153.
58. Potashner SJ, Suneja SK, Benson CG (2000) Altered glycinergic synaptic activities in guinea pig brain stem auditory nuclei after unilateral cochlear ablation. *Hear Res* 147 (1–2):125–136.
59. Suneja SK, Potashner SJ, Benson CG (1998) Plastic changes in glycine and GABA release and uptake in adult brain stem auditory nuclei after unilateral middle ear ossicle removal and cochlear ablation. *Exp Neurol* 151:273–288.
60. Asako M, Holt AG, Griffith RD, Buras ED, Altschuler RA (2005) Deafness-related decreases in glycine-immunoreactive labeling in the rat cochlear nucleus. *J Neurosci Res* 81(1):102–109.
61. Kaltenbach JA, et al. (1998) Changes in spontaneous neural activity in the dorsal cochlear nucleus following exposure to intense sound: Relation to threshold shift. *Hear Res* 124(1–2):78–84.
62. Zhang JS, Kaltenbach JA (1998) Increases in spontaneous activity in the dorsal cochlear nucleus of the rat following exposure to high-intensity sound. *Neurosci Lett* 250:197–200.
63. Brozoski TJ, Bauer CA, Caspary DM (2002) Elevated fusiform cell activity in the dorsal cochlear nucleus of chinchillas with psychophysical evidence of tinnitus. *J Neurosci* 22:2383–2390.
64. Roberts LE, et al. (2010) Ringing ears: The neuroscience of tinnitus. *J Neurosci* 30: 14972–14979.
65. Schaette R, Kempter R (2006) Development of tinnitus-related neuronal hyperactivity through homeostatic plasticity after hearing loss: A computational model. *Eur J Neurosci* 23:3124–3138.
66. Schaette R, McAlpine D (2011) Tinnitus with a normal audiogram: Physiological evidence for hidden hearing loss and computational model. *J Neurosci* 31:13452–13457.
67. Yang S, Weiner BD, Zhang LS, Cho SJ, Bao S (2011) Homeostatic plasticity drives tinnitus perception in an animal model. *Proc Natl Acad Sci USA* 108:14974–14979.
68. Shore SE, Koehler S, Oldakowski M, Hughes LF, Syed S (2008) Dorsal cochlear nucleus responses to somatosensory stimulation are enhanced after noise-induced hearing loss. *Eur J Neurosci* 27:155–168.